



# Quantifying the volume increase and chemical exchange during serpentinization

Frieder Klein\* and Véronique Le Roux\*

Woods Hole Oceanographic Institution, Woods Hole, Massachusetts 02543, USA

## ABSTRACT

**Quantifying the concurrent changes in rock volume and fluid composition during serpentinization remains a major challenge in assessing its physicochemical effects during continental rifting, seafloor spreading, and subduction. Here we conducted a series of 11 hydrothermal laboratory experiments where cylindrical cores of natural dunite, harzburgite, and pyroxenite were reacted with an aqueous solution at 300 °C and 35 MPa for up to 18 months. Using three-dimensional microcomputed tomography and thermogravimetry, we show that rock volume systematically increased with time and extent of reaction, leading to a volume increase of 44% ( $\pm 8\%$ ) in altered rock domains after 10–18 months of serpentinization. The volume expansion was accompanied by Mg–Ca exchange between fluid and rock, while Fe and Si were largely conserved. We find that the protolith composition (olivine/orthopyroxene ratio) plays a significant role in controlling the fluid chemistry and the proportions of hydrous secondary minerals during serpentinization. Agreement between alteration mineralogy, composition of reacting fluids, and measured volume changes suggests that serpentinization under static conditions is a volume-increasing process in spite of demonstrable mass transfer. Volume expansion implies an increased water carrying capacity and buoyancy force of serpentinite per unit mass of protolith, while Mg–Ca exchange during serpentinization may affect the Mg/Ca ratio of seawater on Earth and possibly other ocean worlds.**

## INTRODUCTION

Serpentinite forms when Mg- and Fe-rich rocks (e.g., peridotite) interact with aqueous fluids at temperatures below ~400 °C (Klein et al., 2013). Because of its widespread occurrence at mid-ocean ridges, passive margins, and subduction zones and its high water content, low density, and rheological properties, serpentinite is recognized as a key player in the global water cycle and plate tectonic processes (Guillot and Hattori, 2013). For instance, serpentinite is considered to be one of the main water carriers into subduction zones (Rüpke et al., 2004; Hacker, 2008). There, the low density of serpentinite can facilitate mud volcanism or even eclogite exhumation, whereas dehydration of serpentinite may cause earthquakes, flux melting, and arc volcanism (Hacker et al., 2003; Gerya and Yuen, 2007; Fryer, 2012; Hirth and Guillot, 2013).

The low density and high water content of serpentinite are undisputed, but it is uncertain how much water is consumed during serpentinization per unit mass of peridotite protolith, what the associated volume changes are, if any, and whether major element compositions are modified to significant extents beyond the well-established loss of Ca. Serpentinization is commonly treated as a quasi-isochemical process except for the addition of water and loss of Ca, with an inferred volume increase ranging from 25% to >50%. Fracture patterns, thermodynamic calculations, and the general lack of field evidence for mass transfer of Mg, Si, and Fe in country rocks are cited to support this idea (O’Hanley, 1992; Evans, 2004; Plümper et al., 2012; Rouméon and Cannat, 2014; Malvoisin, 2015; de Obeso and Kelemen, 2018). In contrast, other studies have argued that serpentinization is a volume-for-volume process, accommodated by removal of 30% rock mass, a suggestion that rests on

pseudomorphic replacement textures, the apparent lack of deformation on a microscopic scale, and modified major element ratios in serpentinites (Lindgren, 1918; Thayer, 1966; Putnis and Austrheim, 2010; Velbel, 2014). These conflicting interpretations emphasize the question as to whether the decrease in rock density during serpentinization is accommodated by an increase in rock volume, a massive export of major elements, or a combination of both. The resulting lack of certainty has made it difficult to rigorously quantify geochemical and geodynamic effects of serpentinization, which is why precise and novel measurements are needed. Hence, the overarching goal of our study is to quantify the volume changes of serpentinization and concomitant changes in fluid chemistry using a series of hydrothermal laboratory experiments, conducted under well-constrained conditions.

## MATERIALS AND METHODS

Eleven (11) unaltered cylindrical cores of harzburgite ( $n = 8$ ), dunite ( $n = 2$ ), and pyroxenite ( $n = 1$ ) from Meerfelder Maar (Eifel, Germany, 50.1008°N, 6.7575°E; experiments 1–6) and Twin Sisters massif (Washington State, USA, 48°42'16"N, 121°59'15"W; experiments 7–12) were chosen to cover a range of protolith compositions affected by serpentinization. Cores were scanned with X-ray microcomputed tomography (micro-CT) before each experiment (Fig. 1; Figs. DR1 and DR2 in the GSA Data Repository<sup>1</sup>), and modal proportions of primary minerals (Table DR1) were extracted using the software package Avizo (<https://www.thermofisher.com/us/en/home/industrial/electron-microscopy/electron-microscopy-instruments-workflow-solutions/3d-visualization-analysis-software/avizo-materials-science.html>). Individual rock cores were then reacted

\*Both authors contributed equally to this study.

<sup>1</sup>GSA Data Repository item 2020156, description of analytical details, Figures DR1–DR5, and Tables DR1 and DR2, is available online at <http://www.geosociety.org/datarepository/2020/>, or on request from [editing@geosociety.org](mailto:editing@geosociety.org).

CITATION: Klein, F., and Le Roux, V., 2020, Quantifying the volume increase and chemical exchange during serpentinization: *Geology*, v. 48, p. , <https://doi.org/10.1130/G47289.1>

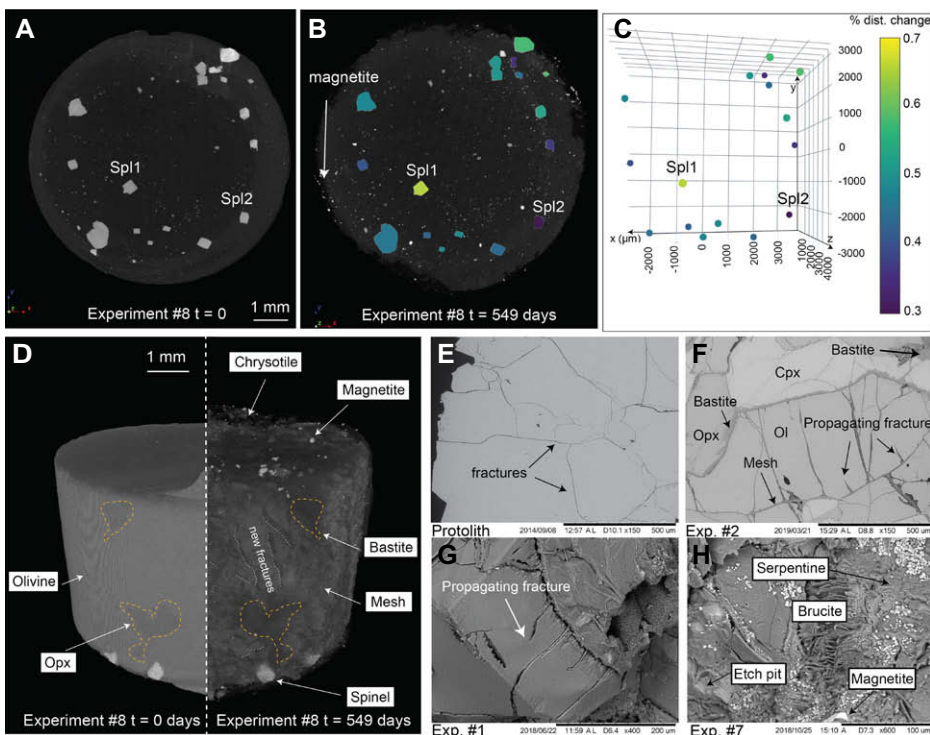


**Figure 1.** (A, B) Microcomputed tomography Z-stacked view of fresh (A) and serpentinized (B) harzburgite from the Twin Sisters massif (Washington State, USA, 48°42'16"N, 121°59'15"W). Color code reflects the average distance change between a spinel and all other spinels, after the reaction (color scale as in C). (C) Centroid positions of spinels shown in B in three-dimensional (3-D) coordinate system (axis labels are in micrometers). (D) Mirrored 3-D rendering of fresh (left) and serpentinized (right) peridotite half-sections (see Fig. DR1 [see footnote 1] for radiograph). Opx—orthopyroxene. (E–H) Backscattered electron images: unaltered protolith with preexisting fractures from Meerfelder Maar (Eifel, Germany, 50.1008°N, 6.7575°E) (E); pseudomorphic mesh texture after olivine (Ol), and bastite texture after orthopyroxene (Opx), and clinopyroxene (Cpx) (F) fractures extending from etch pits in olivine (Meerfelder Maar) (F, G); and secondary minerals on pitted olivine surface (H) in partially serpentinized harzburgite from Twin Sisters.

with an aqueous fluid of seawater salinity (Table DR2) in gold capsules at 300 °C and 35 MPa for periods of 5, 10, and 18 months. The water-to-rock mass ratio of the reactants ranged from 0.80 to 1.87. After terminating the experiments, fluids were analyzed by inductively coupled plasma–mass spectrometry (ICP-MS). Reacted rocks were scanned with micro-CT (Fig. 1; Figs. DR1 and DR2) before they were cut into three pieces each. One end piece was made into two to three petrographic thin sections at High Mesa Petrographics (Los Alamos, New Mexico, USA), and a 1–2-mm-thick center piece was ground for thermogravimetry. The remaining material is stored at the Woods Hole Oceanographic Institution (Massachusetts, USA). The alteration mineralogy was characterized by means of confocal Raman spectroscopy, optical microscopy, and scanning electron microscopy (SEM). Thermogravimetry was used to determine the extent of alteration and molar proportions of hydrous secondary minerals.

Changes in rock volume were calculated using the positions of spinel grains in micro-CT scans before and after the experiment (Fig. 1). Volume calculations were performed

using 17–83 spinels per sample, each ~100–500  $\mu\text{m}$  in size. The position of each spinel centroid was used to calculate its distance to the centroid of all other spinels as

$$d_{\text{Spl1-Spl2}} = \sqrt{(x_2 - x_1)^2 + (y_2 - y_1)^2 + (z_2 - z_1)^2}, \quad (1)$$

where  $d_{\text{Spl1-Spl2}}$  is the distance between spinel 1 and spinel 2, and  $x$ ,  $y$ , and  $z$  are their respective three-dimensional coordinates. Distances between spinel pairs in the protolith were subtracted from distances between spinel pairs in the reacted rocks to calculate distance changes (%). Distance changes were recalculated to volume changes:

$$\Delta V = \{\pi \times [r + (r \times d\%)]^2 \times [h + (h \times d\%)]\} - [\pi \times r^2 \times h], \quad (2)$$

where  $r$  is radius and  $h$  is height. Details of all analytical protocols are provided in the Data Repository.

## CHANGES IN ROCK VOLUME

Overall rock volumes increased by 0.7%–2.2% and correlated with experimental duration, extent of reaction, and fluid composition (Figs. 2 and 3). Averaged rates of volume increase were  $3.2\% \times 10^{-3}$  per day (Table DR1). Volume changes in the reacted rock portions, i.e., excluding the relict protolith, quantified by normalizing the overall volume change in the sample by the extent of reaction for each experiment, were 20% ( $\pm 12\%$ ) after 5 months, and 44% ( $\pm 8\%$ ) after 10–18 months of serpentinization (Fig. 2). The more-limited volume increase during the first 5 months is likely due to nucleation and growth of secondary minerals in pore spaces between primary minerals rather than export of mass. At 10–18 months of reaction, the average volume increase of 44% is close to the predicted volume increase if major elements released by dissolution of primary minerals were largely conserved in the newly formed serpentine (Hostetler et al., 1966; Barnes and O'Neil, 1969; Coleman and Keith, 1971).

## CHANGES IN FLUID CHEMISTRY

Fluid compositions do not show significant enrichments in major elements except for Ca (Fig. 3; Fig. DR3; Table DR1), which is consistent with previous studies (e.g., Seyfried et al., 2007; McCollom et al., 2016). Mass balance of Si and Fe in the reactant fluid and secondary minerals suggests that >99 wt% of these elements released from the dissolving peridotite were taken up by serpentine. Increasing concentrations of dissolved Ca were mirrored by proportionally decreasing concentrations of dissolved Mg (Fig. 3), suggesting Mg–Ca exchange between reactant fluid and serpentinizing peridotite. The search for the underlying cause of Mg–Ca exchange revealed that the Mg/Ca ratio of fluids correlated with—and were thus likely controlled by—the modal olivine/orthopyroxene ratio of the protolith (Fig. 3). Likewise, dissolved Si decreased with increasing olivine:orthopyroxene, which underscores the importance of protolith composition in regulating the fluid chemistry (Fig. 3). Everything considered, the loss of Ca from the rock was compensated by Mg gain, and because Fe and Si were largely conserved in serpentine, changes in fluid chemistry had no discernable effect on rock volume.

## CLUES FROM SOLID REACTION PRODUCTS

Rocks showed extensive signs of alteration on the rock exteriors and interiors, including secondary minerals, dissolution pits, and fractures (Fig. 1; Fig. DR4). Fractures are filled with secondary minerals, and the density of the fracture network increased with time. Accordingly, these fractures formed during serpentinization and not during (de)pressurization (Fig. 1; Fig. DR2). Approximately 1.8–5.5 wt% of the protoliths

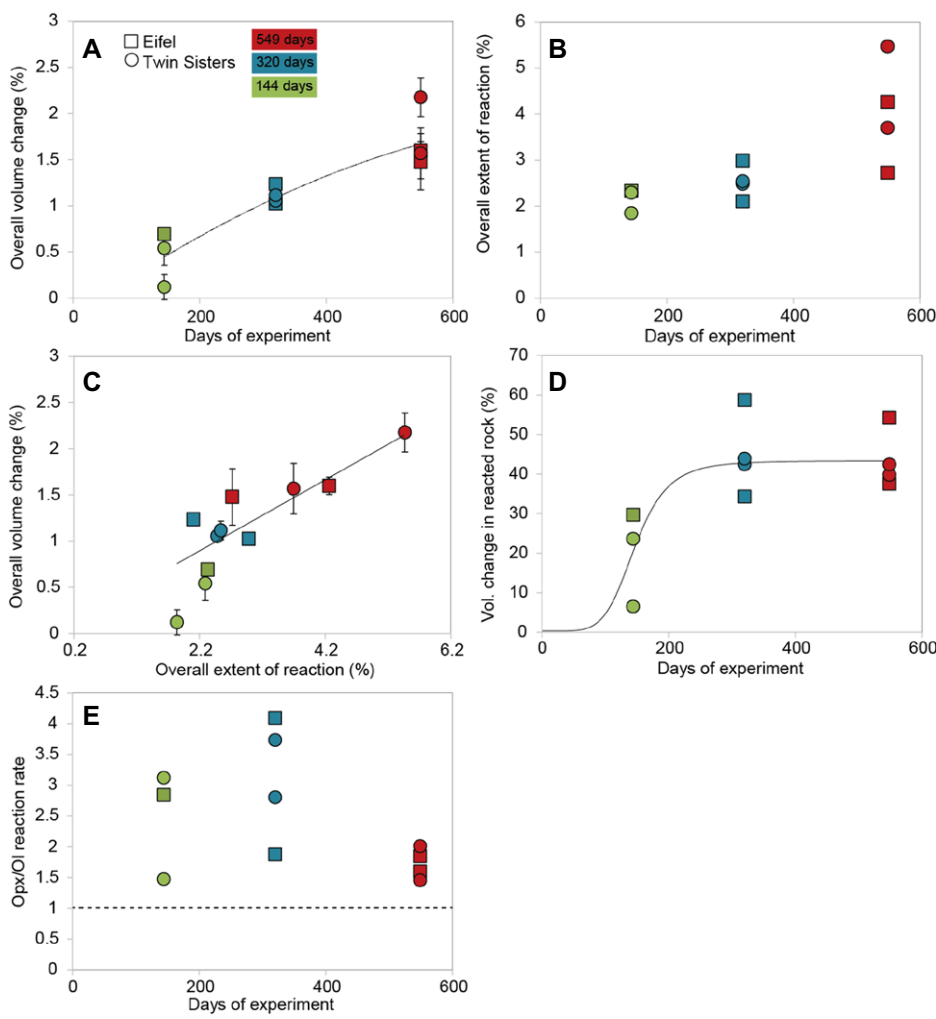
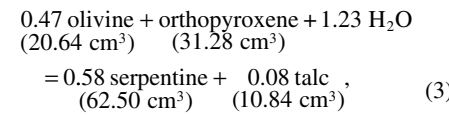


**Figure 2.** (A,B) Overall volume changes (A) and extents of reaction (B, wt% protolith) increase with time. (C) Overall volume changes increase with extent of reaction. (D) Average volume increase in reacted rock portions is 44% after 10–18 months. (E) Orthopyroxene/olivine (Opx/OI) reaction-rate ratios as function of time. Samples are from Meerfelder Maar (Eifel, Germany, 50.1008°N, 6.7575°E) and Twin Sisters massif (Washington State, USA, 48°42'16"N, 121°59'15"W).

reacted during the experiments (Fig. 4), and extents of reaction increased with time and volume increase (Figs. 2 and 4). The average extent of reaction was  $1.5 \times 10^{-2}$  wt% per day (in terms of protolith reacted) after 5 months, and subsequently decreased to  $7.4 \times 10^{-3}$  wt% per day after 18 months (Table DR1). In comparison with studies that used powdered reactants (Seyfried et al., 2007; McCollom et al., 2016), the lower extent of reaction per unit of time has been attributed to more-restricted fluid pathways and smaller surface areas of natural rocks (Malvoisin and Brunet, 2014; Klein et al., 2015).

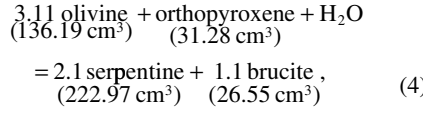
Serpentinization of pyroxene-rich harzburgite and pyroxenite (experiments 1–6) resulted in the precipitation of lizardite, chrysotile, talc, and minor magnetite (Fig. 1; Figs. DR4 and DR5). Because Mg, Fe, and Si were conserved in serpentinite, it was possible to use the molar proportions of hydrous secondary minerals as derived from thermogravimetry (Fig. 4; Table DR1) to estimate the molar proportions of oliv-

ine and orthopyroxene that underwent serpentinization. This provides an independent assessment of volume changes. The simplified reaction



suggests an average volume increase of ~41% in experiments 1–6.

Serpentinization of pyroxene-poor harzburgite and dunite (experiments 7–12) resulted in the formation of lizardite, chrysotile, brucite, and minor magnetite (Fig. 1; Figs. DR4 and DR5). Based on the abundances of serpentine and brucite in the reaction products, the simplified reaction



suggests an average volume increase of 49% in experiments 7–12. The proportions of olivine in the protoliths (Table DR1) were higher than Equations 3 and 4 suggest, but this discrepancy can be reconciled if orthopyroxene reacted 1.5x–4.1x faster than olivine at the experimental conditions (Fig. 2). Indeed, orthopyroxene is surrounded by significantly thicker reaction halos than olivine (Fig. DR4), suggesting that its alteration is more efficient at the experimental conditions. Within analytical uncertainties, the average volume changes independently derived from the alteration mineralogy of experiments 1–12 in Equations 3 and 4 agree with volume increases measured by micro-CT.

## PHYSICOCHEMICAL IMPLICATIONS

The results presented here substantiate interpretations that serpentinization is a volume-increasing process (Hostetler et al., 1966; Coleman and Keith, 1971; O'Hanley, 1992); nonetheless, we show that serpentinization is by no means isochemical and the ensuing physicochemical implications are extensive. An immediately apparent implication of the volume increase is the higher capacity of serpentinite to take on water per unit mass of peridotite. If serpentinization of 1 m<sup>3</sup> of peridotite yields 1.44 m<sup>3</sup> of serpentinite with a density of 2.60 g/cm<sup>3</sup>, 468 kg of water must be added, whereas isovolumetric serpentinization of 1 m<sup>3</sup> peridotite would consume only 325 kg water. The volume increase also entails a stronger net buoyancy force, which scales linearly with the addition of water. This effect promotes diapiric ascent of serpentinite and can, for instance, facilitate mud volcanism, the exhumation of subducted terranes, and arc volcanism (Fryer, 2012; Guillot and Hattori, 2013). In addition to extrusion of buoyant serpentinite, the increased rock volume may express itself through increased surface elevation and increased rates of surface erosion (Kelemen and Hirth, 2012).

Hydrothermal vent fluids influenced by serpentinization are depleted in Mg and enriched in Ca relative to seawater while other major elements show conservative behavior (e.g., Seyfried et al., 2015). Measured fluid compositions of these and previous hydrothermal laboratory experiments, including those conducted under open-system conditions (Normand et al., 2002; Godard et al., 2013; Escario et al., 2018), also reveal conservation of major elements, except for Ca, within the serpentinizing rock. Fluid compositions hence further corroborate an increase in rock volume in both open and closed serpentinization systems. Whereas the uptake of Mg by serpentinite in exchange for Ca has a negligible effect on rock volume, it may cause a discernable decrease in seawater Mg/Ca during periods of widespread peridotite exposure, such as during

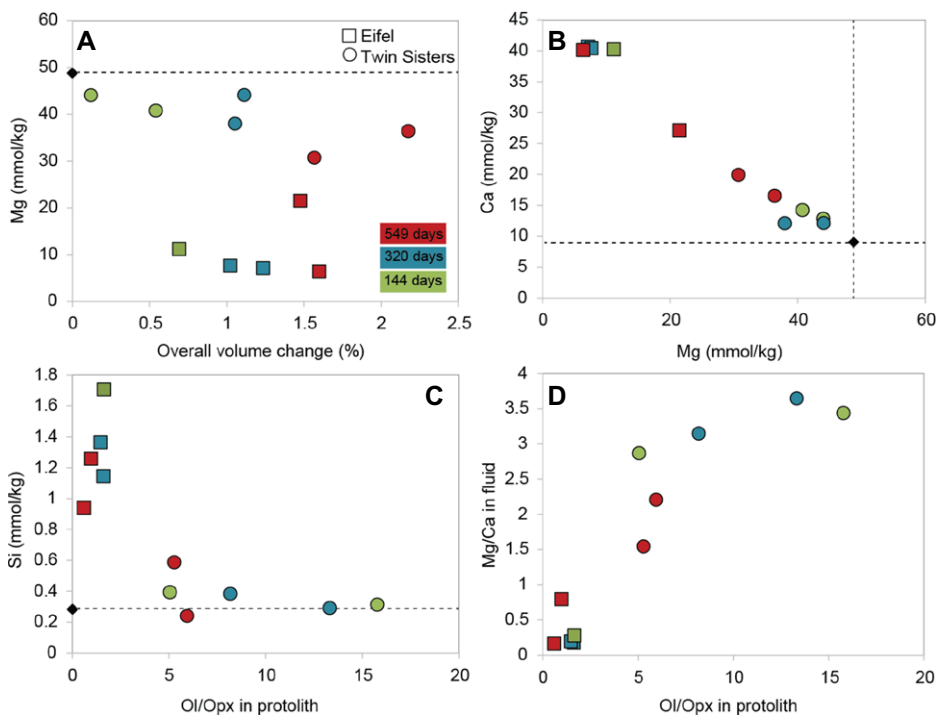


**Figure 3.** (A) Concentrations of dissolved Mg decrease with increasing rock volume. (B) Increasing concentrations of dissolved Ca mirrored by decreasing Mg-for-Ca exchange. (C,D) Dissolved Si (C) and Mg/Ca ratios in fluids (D) vary with the modal olivine (OI) / orthopyroxene (Opx) ratio, indicating the first-order influence of protolith composition on fluid chemistry. Colors refer to experiment durations. Samples are from Meerfelder Maar (Eifel, Germany, 50.1008°N, 6.7575°E) and Twin Sisters massif (Washington State, USA, 48°42'16"N, 121°59'15"W). Dashed lines and black diamonds indicate starting fluid concentration; in D, starting Mg/Ca in fluid plots off scale at 5.4.

the breakup of supercontinents, or on “ocean worlds” of the outer solar system where the seafloor is thought to be paved with ultramafic rocks (Vance and Melwani Daswani, 2020).

Our results are most relevant to serpentinization under quasi-static conditions without, or with only limited, fluid flow, although reaction-induced fracturing may allow for transient fluid advection on a micrometer scale. Newly formed fractures observed here (Fig. 1; Fig. DR2) closely resemble those in natural serpentinites attributed to reaction-induced cracking (Kelemen and Hirth, 2012; Plümper et al., 2012). Notwithstanding that serpentinization can decrease permeability, available constraints corroborate the idea that serpentinization is a cyclical process, wherein the volume increase causes fracturing, and the newly created porosity provides fluid access to fresh mineral surfaces, thus allowing serpentinization to run to completion (Kelemen and Hirth, 2012; Plümper et al., 2012; Godard et al., 2013; Farough et al., 2016; Tutolo et al., 2016). Whereas mass is largely conserved in serpentinizing peridotite as a whole, on a millimeter scale, mass transfer of Si and Mg between serpentinizing olivine and pyroxene can be extensive (Klein et al., 2015). Mass transfer may hence result in distinct volume changes in distinct rock domains (Fig. 1), causing strain and promoting cracking.

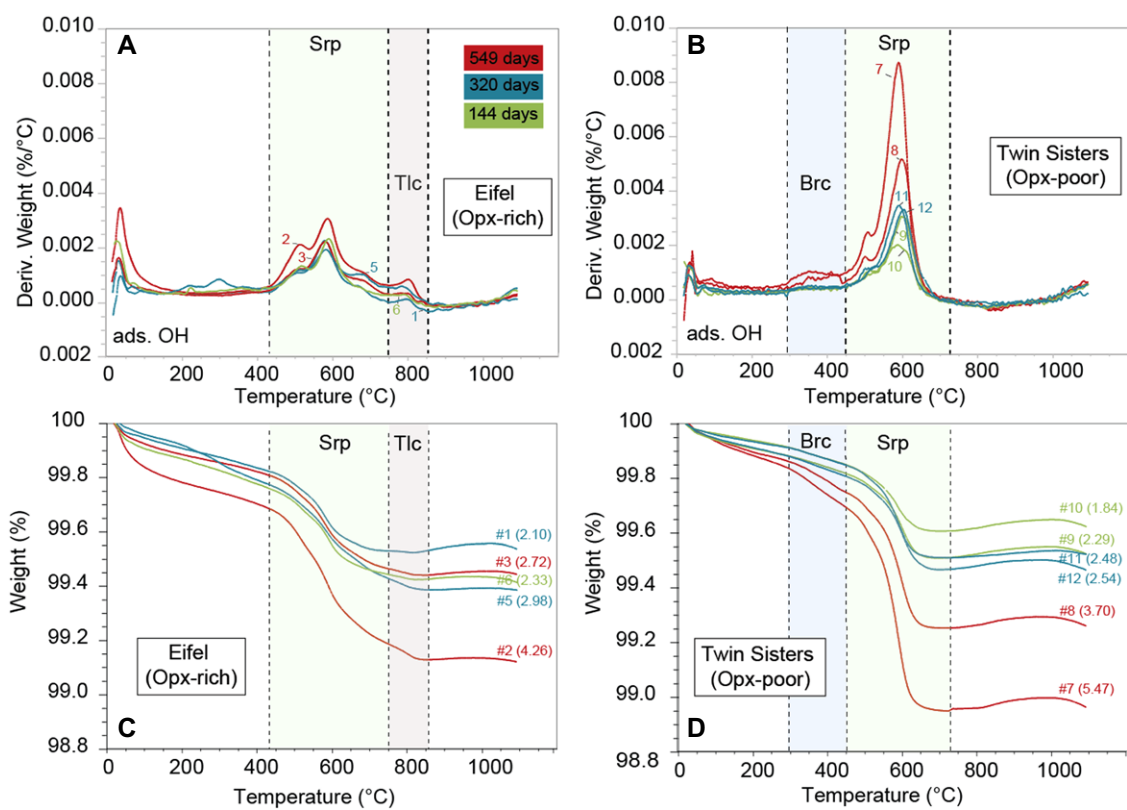


**Figure 4.** Thermogravimetry of reaction products (Opx—orthopyroxene). (A,B) First derivative of weight (deriv. weight) from hydrous minerals as a function of temperature in reacted rocks from Eifel (Meerfelder Maar, Germany, 50.1008°N, 6.7575°E) (A) and Twin Sisters massif (Washington State, USA, 48°42'16"N, 121°59'15"W) (B). Serpentine (Srp), brucite (Brc), and talc (Tlc) show distinct decomposition temperature intervals. (C,D) Weight change of reacted rocks from Eifel (C) and Twin Sisters (D) as a function of temperature. Decrease in weight reflects the loss of water from hydrous minerals during heating, which allows their quantification. Non-bracketed numbers indicate experiment numbers; bracketed numbers indicate weight percent protolith reacted. Colors refer to experiment durations.

Arguably, there is no single value for the volume increase during serpentinization, but average overall volume changes quantified here are close to expected values if mass is largely conserved and Mg–Ca exchange is considered. Taking complementary constraints from thermodynamic calculations (Kelemen and Hirth, 2012; Malvoisin, 2015; de Obeso and Kelemen, 2018), hydrothermal experiments (Seyfried et al., 2007; Godard et al., 2013; McCollom et al., 2016; Escario et al., 2018), and field studies (Hostettler et al., 1966; Coleman and Keith, 1971; Charlou et al., 2002; Seyfried et al., 2015) into consideration, our results suggest a volume increase of 40%–45% for serpentinization at mid-ocean ridges, passive margins, and subduction-zone forearcs.

## ACKNOWLEDGMENTS

We thank P. Kelemen, O. Plümper, an anonymous reviewer, and editor C. Clark, whose constructive comments helped to improve this article. This study was supported by U.S. National Science Foundation award 1551431 to Klein and Le Roux.

## REFERENCES CITED

Barnes, I., and O’Neil, J.R., 1969, The relationship between fluids in some fresh alpine-type ultramafics and possible modern serpentinization, western United States: Geological Society of America Bulletin, v. 80, p. 1947–1960, [https://doi.org/10.1130/0016-7606\(1969\)80\[1947:TRBFIS\]2.0.CO;2](https://doi.org/10.1130/0016-7606(1969)80[1947:TRBFIS]2.0.CO;2).

Charlou, J.-L., Donval, J.-P., Fouquet, Y., Jean-Baptiste, P., and Holm, N., 2002, Geochemistry of high  $H_2$  and  $CH_4$  vent fluids issuing from ultramafic rocks at the Rainbow hydrothermal field ( $36^{\circ}14'N$ , MAR): Chemical Geology, v. 191, p. 345–359, [https://doi.org/10.1016/S0009-2541\(02\)00134-1](https://doi.org/10.1016/S0009-2541(02)00134-1).

Coleman, R.G., and Keith, T.E., 1971, A chemical study of serpentinization, Burro Mountain, California: Journal of Petrology, v. 12, p. 311–328, <https://doi.org/10.1093/petrology/12.2.311>.

de Obeso, J.C., and Kelemen, P.B., 2018, Fluid–rock interactions on residual mantle peridotites overlain by shallow oceanic limestones: Insights from Wadi Fins, Sultanate of Oman: Chemical Geology, v. 498, p. 139–149, <https://doi.org/10.1016/j.chemgeo.2018.09.022>.

Escario, S., Godard, M., Gouze, P., and Leprovost, R., 2018, Experimental study of the effects of solute transport on reaction paths during incipient serpentinization: Lithos, v. 323, p. 191–207, <https://doi.org/10.1016/j.lithos.2018.09.020>.

Evans, B.W., 2004, The serpentine multisystem revisited: Chrysotile is metastable: International Geology Review, v. 46, p. 479–506, <https://doi.org/10.2747/0020-6814.46.6.479>.

Farough, A., Moore, D.E., Lockner, D.A., and Lowell, R.P., 2016, Evolution of fracture permeability of ultramafic rocks undergoing serpentinization at hydrothermal conditions: An experimental study: Geochemistry Geophysics Geosystems, v. 17, p. 44–55, <https://doi.org/10.1002/2015GC005973>.

Fryer, P., 2012, Serpentinite mud volcanism: Observations, processes, and implications: Annual Review of Marine Science, v. 4, p. 345–373, <https://doi.org/10.1146/annurev-marine-120710-100922>.

Gerya, T.V., and Yuen, D.A., 2007, Robust characteristics method for modelling multiphase visco-elasto-plastic thermo-mechanical problems: Physics of the Earth and Planetary Interiors, v. 163, p. 83–105, <https://doi.org/10.1016/j.pepi.2007.04.015>.

Godard, M., Luquot, L., Andreani, M., and Gouze, P., 2013, Incipient hydration of mantle lithosphere at ridges: A reactive-percolation experiment: Earth and Planetary Science Letters, v. 371–372, p. 92–102, <https://doi.org/10.1016/j.epsl.2013.03.052>.

Guillot, S., and Hattori, K., 2013, Serpentinites: Essential roles in geodynamics, arc volcanism, sustainable development, and the origin of life: Elements, v. 9, p. 95–98, <https://doi.org/10.2113/gselements.9.2.95>.

Hacker, B.R., 2008,  $H_2O$  subduction beyond arcs: Geochemistry Geophysics Geosystems, v. 9, Q03001, <https://doi.org/10.1029/2007GC001707>.

Hacker, B.R., Peacock, S.M., Abers, G.A., and Holloway, S.D., 2003, Subduction factory 2. Are intermediate-depth earthquakes in subducting slabs linked to metamorphic dehydration reactions?: Journal of Geophysical Research, v. 108, 2030, <https://doi.org/10.1029/2001JB001129>.

Hirth, G., and Guillot, S., 2013, Rheology and tectonic significance of serpentinite: Elements, v. 9, p. 107–113, <https://doi.org/10.2113/gselements.9.2.107>.

Hostettler, P.B., Coleman, R.G., Mumpum, F.A., and Evans, B.W., 1966, Brucite in alpine serpentinites: American Mineralogist, v. 51, p. 75–98.

Kelemen, P.B., and Hirth, G., 2012, Reaction-driven cracking during retrograde metamorphism: Olivine hydration and carbonation: Earth and Planetary Science Letters, v. 345–348, p. 81–89, <https://doi.org/10.1016/j.epsl.2012.06.018>.

Klein, F., Bach, W., and McCollom, T.M., 2013, Compositional controls on hydrogen generation during serpentinization of ultramafic rocks: Lithos, v. 178, p. 55–69, <https://doi.org/10.1016/j.lithos.2013.03.008>.

Klein, F., Grozeva, N.G., Seewald, J.S., McCollom, T.M., Humphris, S.E., Moskowitz, B., Berqué, T.S., and Kahl, W.-A., 2015, Experimental constraints on fluid–rock interactions during incipient serpentinization of harzburgite: American Mineralogist, v. 100, p. 991–1002, <https://doi.org/10.2138/am-2015-5112>.

Lindgren, W., 1918, Volume changes in metamorphism: The Journal of Geology, v. 26, p. 542–554, <https://doi.org/10.1086/622615>.

Malvoisin, B., 2015, Mass transfer in the oceanic lithosphere: Serpentinization is not isochemical: Earth and Planetary Science Letters, v. 430, p. 75–85, <https://doi.org/10.1016/j.epsl.2015.07.043>.

Malvoisin, B., and Brunet, F., 2014, Water diffusion–transport in a synthetic dunite: Consequences for oceanic peridotite serpentinization: Earth and Planetary Science Letters, v. 403, p. 263–272, <https://doi.org/10.1016/j.epsl.2014.07.004>.

McCollom, T.M., Klein, F., Robbins, M., Moskowitz, B., Berqué, T.S., Jóns, N., Bach, W., and Templeton, A., 2016, Temperature trends for reaction rates, hydrogen generation, and partitioning of iron during experimental serpentinization of olivine: Geochimica et Cosmochimica Acta, v. 181, p. 175–200, <https://doi.org/10.1016/j.gca.2016.03.002>.

Normand, C., Williams-Jones, A.E., Martin, R.F., and Vali, H., 2002, Hydrothermal alteration of olivine in a flow-through autoclave: Nucleation and growth of serpentine phases: American Mineralogist, v. 87, p. 1699–1709, <https://doi.org/10.2138/am-2002-11-1220>.

O’Hanley, D.S., 1992, Solution to the volume problem in serpentinization: Geology, v. 20, p. 705–708, [https://doi.org/10.1130/0091-7613\(1992\)020<0705:STTVPI>2.3.CO;2](https://doi.org/10.1130/0091-7613(1992)020<0705:STTVPI>2.3.CO;2).

Plümper, O., Røyne, A., Magrasó, A., and Jamtveit, B., 2012, The interface-scale mechanism of reaction-induced fracturing during serpentinization: Geology, v. 40, p. 1103–1106, <https://doi.org/10.1130/G33390.1>.

Putnis, A., and Austrheim, H., 2010, Fluid-induced processes: Metasomatism and metamorphism: Geofluids, v. 10, p. 254–269, <https://doi.org/10.1111/j.1468-8123.2010.00285.x>.

Rouméjon, S., and Cannat, M., 2014, Serpentinization of mantle-derived peridotites at mid-ocean ridges: Mesh texture development in the context of tectonic exhumation: Geochemistry Geophysics Geosystems, v. 15, p. 2354–2379, <https://doi.org/10.1002/2013GC005148>.

Rüpke, L.H., Morgan, J.P., Hort, M., and Connolly, J.A.D., 2004, Serpentine and the subduction zone water cycle: Earth and Planetary Science Letters, v. 223, p. 17–34, <https://doi.org/10.1016/j.epsl.2004.04.018>.

Seyfried, W.E., Jr., Foustoukos, D.I., and Fu, Q., 2007, Redox evolution and mass transfer during serpentinization: An experimental and theoretical study at 200 °C, 500 bar with implications for ultramafic-hosted hydrothermal systems at mid-ocean ridges: Geochimica et Cosmochimica Acta, v. 71, p. 3872–3886, <https://doi.org/10.1016/j.gca.2007.05.015>.

Seyfried, W.E., Jr., Pester, N.J., Tutolo, B.M., and Ding, K., 2015, The Lost City hydrothermal system: Constraints imposed by vent fluid chemistry and reaction path models on subseafloor heat and mass transfer processes: Geochimica et Cosmochimica Acta, v. 163, p. 59–79, <https://doi.org/10.1016/j.gca.2015.04.040>.

Thayer, T.P., 1966, Serpentinization considered as a constant-volume metasomatic process: American Mineralogist, v. 51, p. 685–710.

Tutolo, B.M., Mildner, D.F.R., Gagnon, C.V.L., Saar, M.O., and Seyfried, W.E., Jr., 2016, Nanoscale constraints on porosity generation and fluid flow during serpentinization: Geology, v. 44, p. 103–106, <https://doi.org/10.1130/G37349.1>.

Vance, S.D., and Melwani Daswani, M., 2020, Serpentinite and the search for life beyond Earth: Philosophical Transactions of the Royal Society: A, Mathematical, Physical and Engineering Sciences, v. 378, p. 20180421, <https://doi.org/10.1098/rsta.2018.0421>.

Velbel, M.A., 2014, Stoichiometric reactions describing serpentinization of anhydrous primary silicates: A critical appraisal, with application to aqueous alteration of chondrule silicates in CM carbonaceous chondrites: Clays and Clay Minerals, v. 62, p. 126–136, <https://doi.org/10.1346/CCMN.2014.0620205>.

Printed in USA